# CHAPTER III

# COMPUTATIONAL TECHNIQUES

In this chapter, we will describe the design and development of the algorithm for the probe measurement and the plasma-parameter analysis. Techniques and problems in analyzing such parameters for the manual and automated programs will be given in detail. The simulation model for accuracy tests will also be exhibited in this chapter. At the end of this chapter, the results of calculation by other commercially available program will be discussed base on the single-probe data.

## 3.1 Electrical Single Probe Measurement and Analysis

LabVIEW programs or virtual instruments (VIs) are useful programs due to their intutively appearances and operations, which contain a comprehensive set of tools for acquiring, analyzing, displaying, and storing data [19]. They consist of different components, such as the front panel, the block diagram, and the icon and connector pane. With these components, one can imitate physical instruments with controller and indicators, or help user in troubleshoot the programming code. Furthermore, LabVIEW can be used to communicate with any devices, such as data acquisition (DAQ), general propose interface bus (GPIB), and serial port (RS-232). This, user can control devices via a computer at a remote distance without monitoring the device in the operation area. The electrical single probe measurement and analysis, in this work, was developed in LabVIEW environment mainly because of its features in creating virtual instruments with GPIB communication.

The design of this program composed of four tab menus, I-V Measuring Operation, Open Measurement File, Manual Analysis, and Automatic Analysis. The first one was developed to perform the cylindrically single-probe measurement. The

open measurement file, which is optional, was created to open up a file obtained from the probe measurement which could be from the I-V measuring operation or from elsewhere. And the last two menus were the plasma analysis programs by the manual and automatic methods. The flow chart of the main loop is showed in figure 3.1.

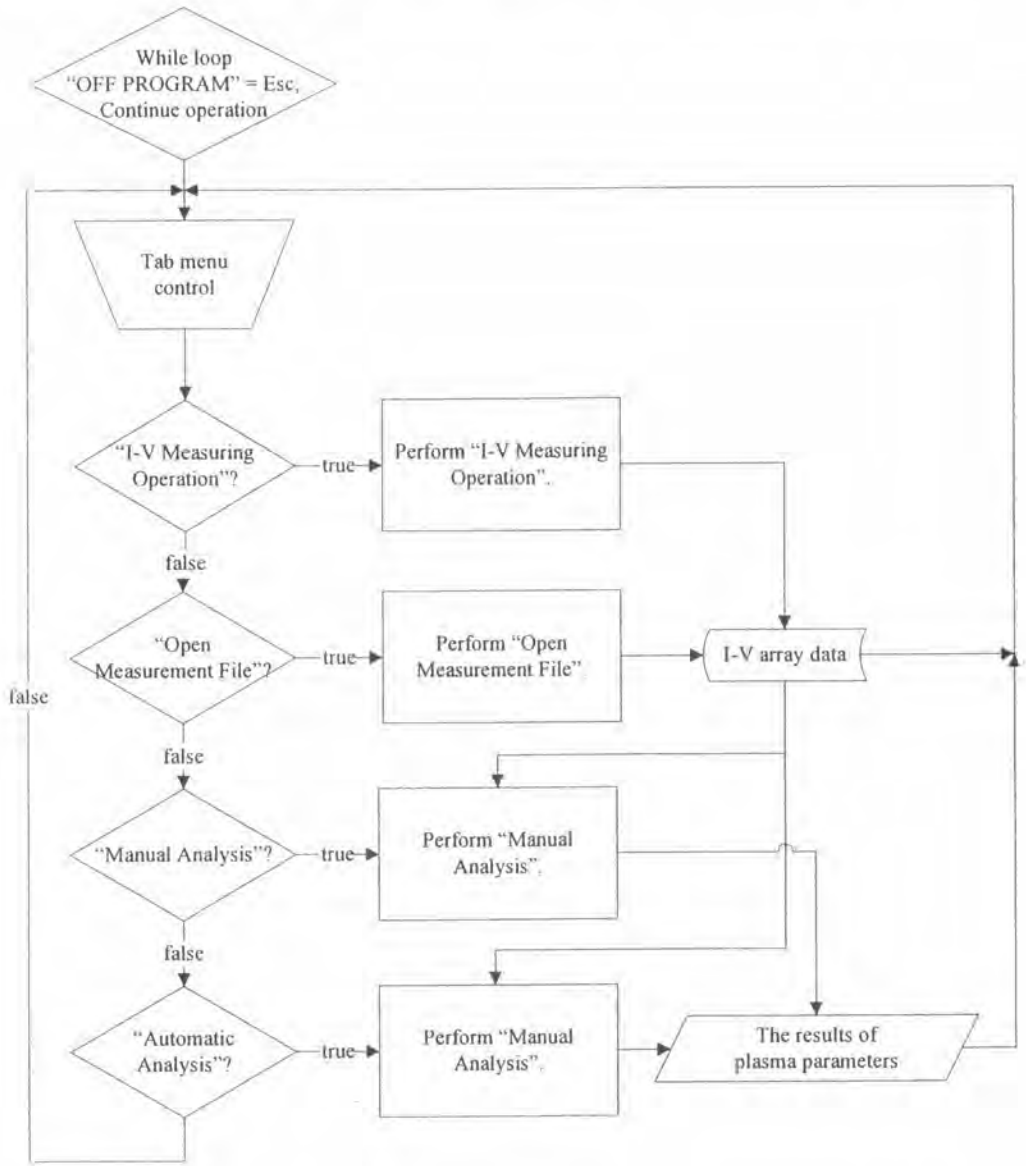


Figure 3.1: The flow chart of the electrical single probe measurement and analysis.

## 3.2 I-V Measuring Operation

This I-V measuring operation was designed to perform the real-time probe measurements of any plasma glow. This program was developed on LabVIEW environment, first to control a voltage source and read a value from current meter, and second to store data and display the result (current-voltage). In the part of controlling the power source, the design of the program has two voltage resolutions because of the electrical characteristic of plasma. The data in the ion and electron saturation regions are needless to have high number of current readings, whereas the currents in the transition region abruptly changing thus need to scan the voltages with high resolution to gain more current information. In other word, the swept voltage would be split into three parts with two resolutions, higher and lower, where the higher resolution lay in the middle of the scanning, according to each regions of the I-V curve (ion-saturation, transition and electron-saturation regions). For the data acquisition, when a probe to which voltages supply gains current flow, the program will read the current corresponding to each voltage. These data will be treated in a two-dimensional array, in which the first and second columns are the voltage and current data respectively, and they are then plotted in the I-V characteristic graph. In this work, the Hewlett Packard (HP) module 4140B was used because it would not only supply voltages (from -100 to +100 V) but also measure currents as well. It, moreover, could communicate with a computer via a GPIB card that was very helpful to transfer and receive data. Figure 3.2 shows the front panel displaying for the user interface of our program.

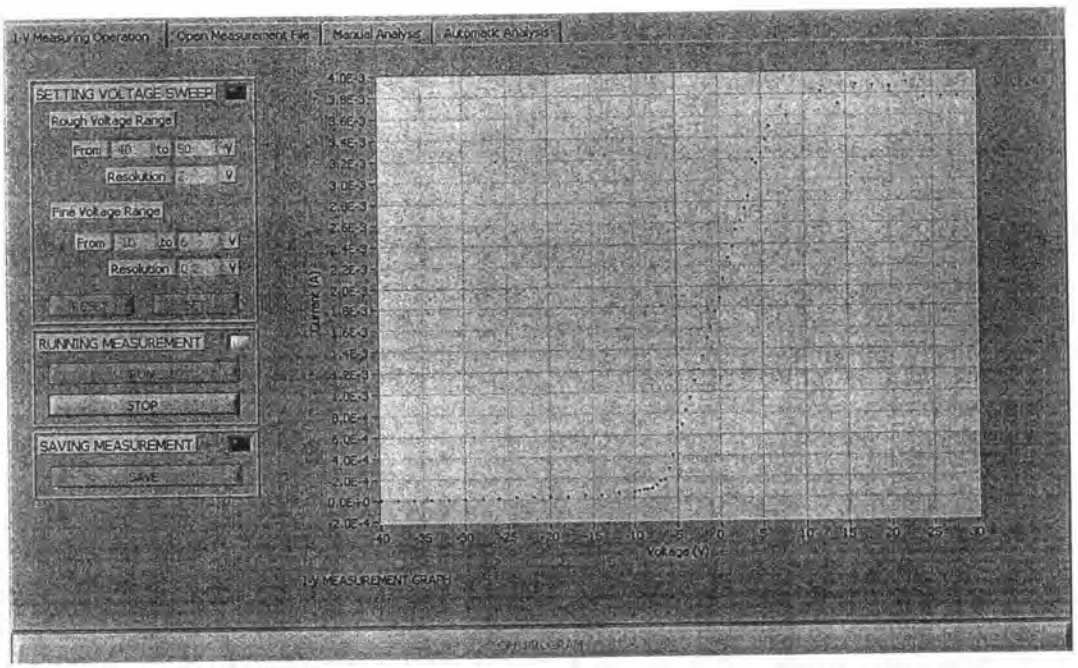


Figure 3.2: The front panel for the user interface.

The appearance of this program can be divided into two sections; that is the controlling section (setting voltage sweep, running measurement and saving measurement) and the display of results (I-V measurement graph). As mentioned above, a user has to input the voltage range and resolutions depending on each I-V range to obtain enough current-voltage data for the analysis, especially the data in the transition region. The next controlling process is the running of measurement. These controls are designed to perform the current-voltage measurement and to stop the ongoing measurement. During the measurement, the current-voltage data will be plotted in the I-V measurement graph. After all, the data will be stored in an array format and then be saved in a file or to be analyzed for the plasma parameters. The flow chart of the I-V measuring operation is illustrated in figure 3.3.

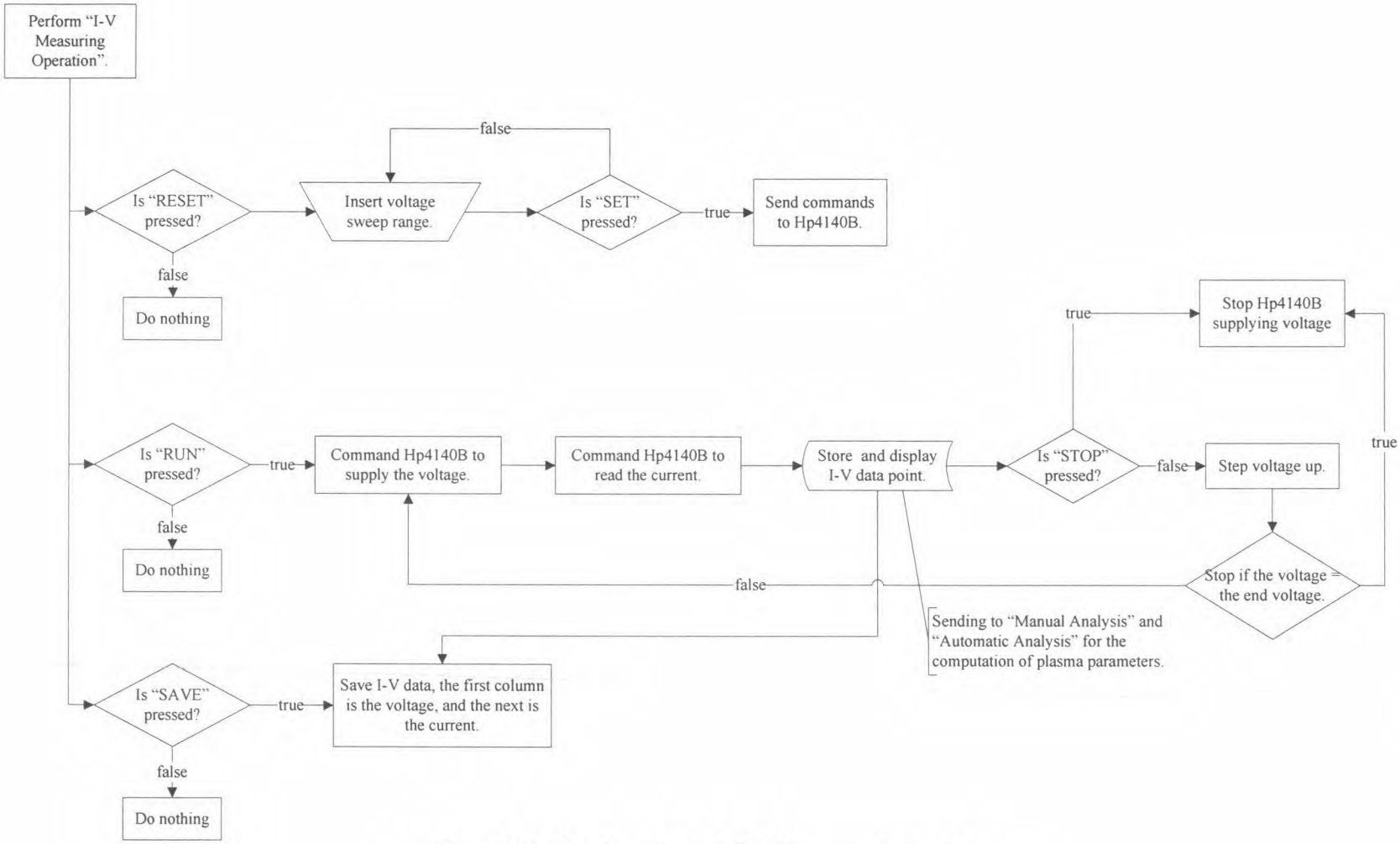


Figure 3.3: The flow chart of the I-V measuring operation.

## 3.3 Open Measurement File

This program is an alternative to help one to analyze the I-V characteristic taken from a file. The two controlling sections that assist one in managing the file before analysis are the multiply factors and the file format. In other single probe systems, currents can be measured in the unit of voltage across a resistor, thus voltages that supply to the probe are basically attenuated. For instance, when one uses an oscilloscope to collect the I-V data, the current is measured across a resistor, and the voltage is measured via voltage divider to avoid the damage of the device. The multiply factors will then manage with these data manipulation by multiplying with an amplification factor to the voltage and dividing the other by the resistor. For the format control, one has to select the format of a file, Text (*.txt or tab delimited) or CSV (*.csv or comma delimited), to read the file properly. Figure 3.4(a) shows the example of a file that was open in this program, and the flow chart of the program is illustrated in figure 3.4(b).

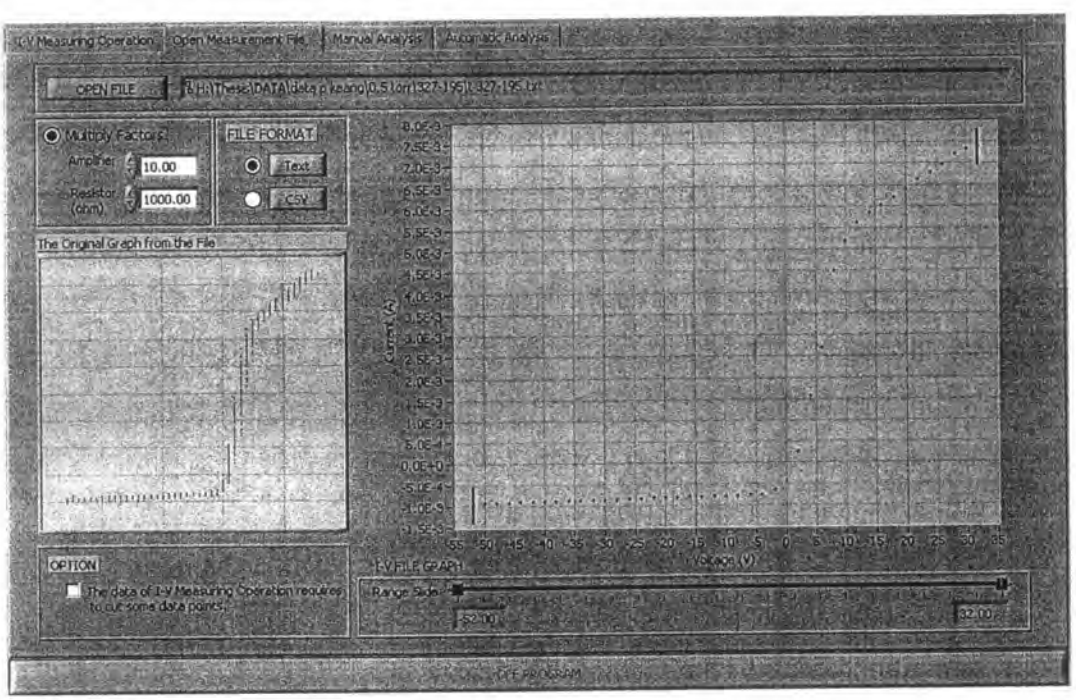


(a)

Figure 3.4: The open measurement file process, (a) an example of the file that is open in the front panel and (b) the flow chart of the program.

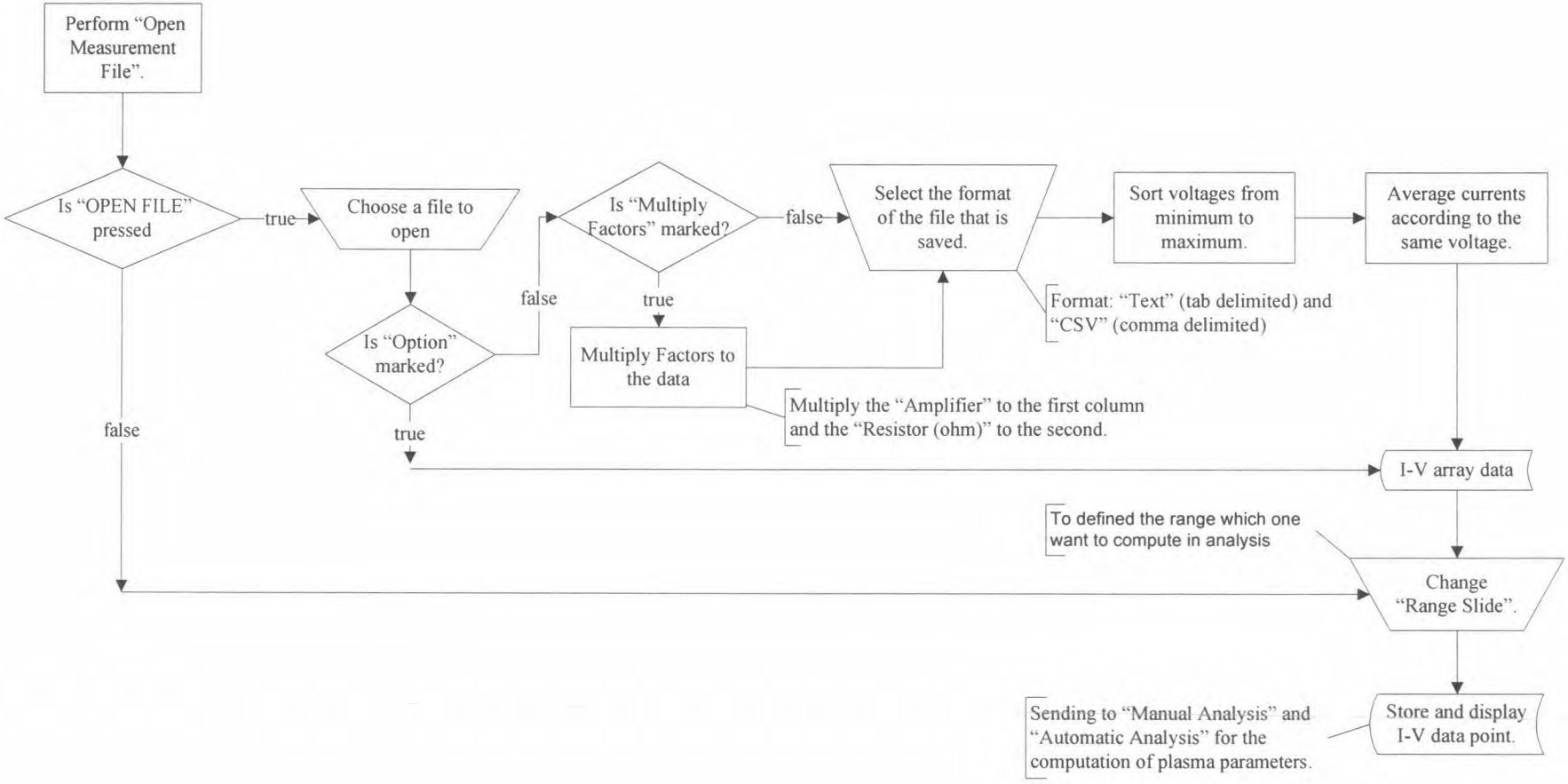


(b)

Figure 3.4: The open measurement file process, (a) an example of the file that is open in the front panel and (b) the flow chart of the program.

Another control adjustment is the range slide bar that lies below the I-V file graph. This bar indicates how long the range is selected; this is to avoid some measured data that have an error in the beginning or end of the measurement. For example, there are some current points in the beginning that overlap or cascade over the other in the ion-saturation region. This causes the miss-estimation of the ion current because of the straight-line fitting will take the error point into account. Using the slide bar, one can avoid the error points from the I-V data by considering the proper range in the I-V file graph, before carrying on the plasma analysis. Also, there is an optional checker that it is designed specifically for the real-time data obtaining from the I-V measuring operation, which sometimes require removal of some error current points.

The advantage of this program is to adjust current data into averaging currents at the same value of voltage. As can be seen in figure 3.4(a), the original graph from the file, for example, showed a problem when a single voltage yielded many discrete measured currents. This problem happened when one used a low resolution oscilloscope collecting the I-V data. In the graph, it is impossible to calculate the first and second derivatives that are mainly used to separate the three regions, which shall be discussed in the automated analysis. Thus in this program, currents at the same voltage have to be averaged, otherwise the manual and automated analysis cannot be analyzed to yield the plasma parameters.

## 3.4 Manual Analysis

The manual analysis imitates steps of the interpretation of the I-V characteristic as the following:

I) Separate the I-V curve into three regions by using the slide bar below the graph of manual separation of three regions in figure 3.5.

II) Compute the plasma potential ($V_p$) and the electron saturation current ($I_{e,sat}$) at the intersection of two straight lines (fittings of the transition interval and of the electron saturation region).

III) Fit the ion current by using the data in the ion-saturation region.

IV) Subtract the ion current out from the I-V data.

V) Re-plot the remaining electron current ($I_e$) with the natural log.

VI) Select the data range of the ln $I_e$-$V$ graph in the previous step to fit a straight line by using the other slide bar on the right side.

VII) Compute the electron temperature ($T_e$) from the inverse slope as in the equation (2.16).

VIII) Calculate the electron ($n_e$) and ion ($n_i$) densities by substituting $T_e$, $I_{e.sat}$, $I_{i.sat}$, the probe area, and the ion mass in the equation (2.17) and (2.18).

The flow chart in figure 3.6 shows the algorithm of the manual analysis.

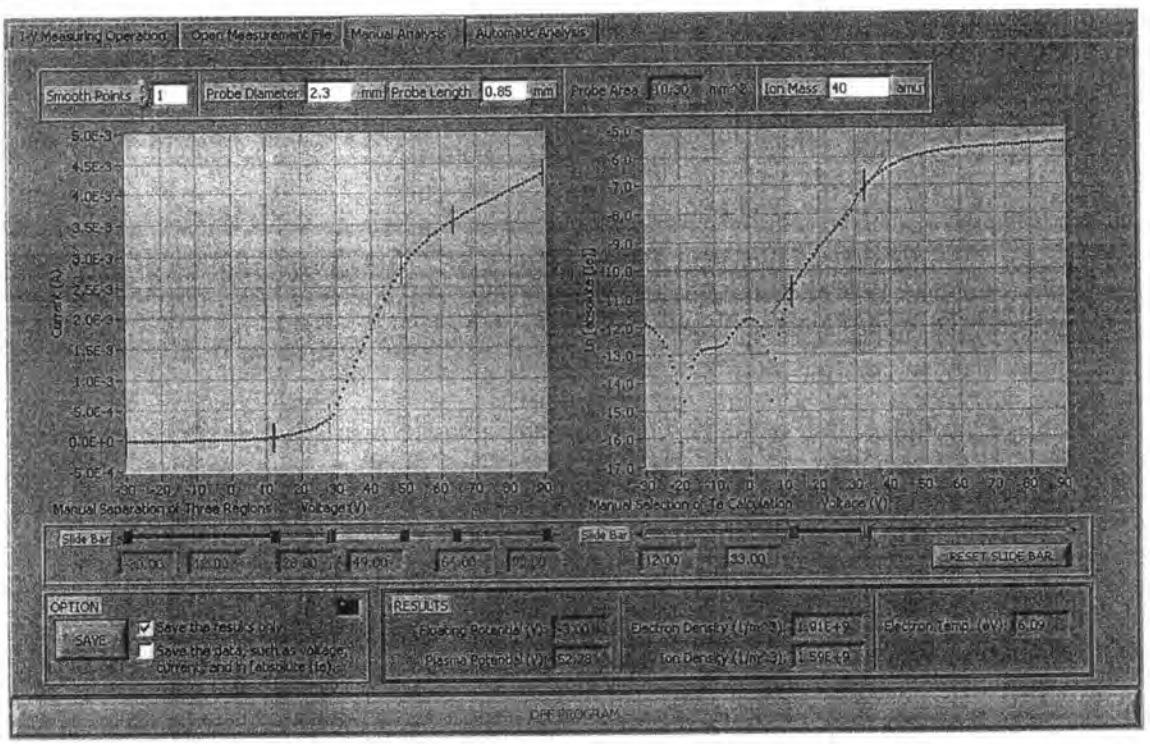


Figure 3.5: The appearance of the manual analysis and the slide bars used as manually defined ranges.

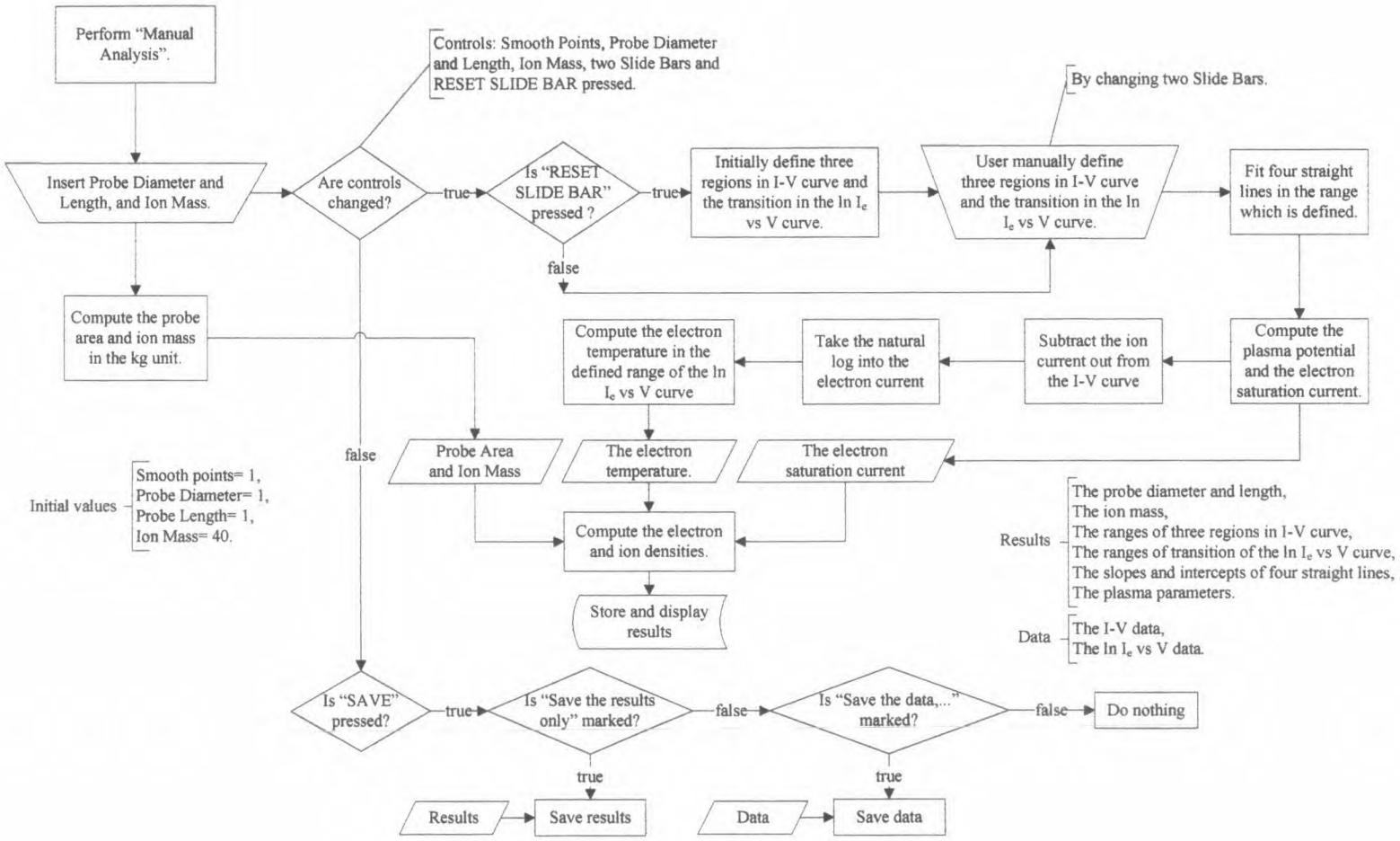


Figure 3.6: The algorithm of the manual analysis.

In figure 3.5, the smooth-points control indicates how many points of data would be averaged. This control will average the adjacent data points to reduce noise or fluctuated data. The more numbers of the smooth points the less noise. The smoothed value at index $i$ is the average of the data points in the interval $[i-(n-1)/2, i+(n-1)/2]$, inclusively, where $n$ is the number of the smooth points. For the expression, the smoothing using adjacent averaging can be written by

$$(V_i, I_i) = (V_i, \frac{I_{i-\frac{n-1}{2}} + \ldots + I_{i-1} + I_i + I_{i+1} + \ldots + I_{i+\frac{n-1}{2}}}{n})$$

where $V$ and $I$ is the voltage and current data, respectively.

The slide bar below the graph of manual separation of three regions was there to define ranges of the ion-saturation, transition, and electron-saturation regions. It consists of six control frets for the beginning and end of each range. The indicator which relates to these slides would be displayed in two ways, one in the graph above this bar showing six frets, and the other below it represents voltage positions. Similarly to the first bar, the second bar is used for the range definition of the manual selection of $T_e$ calculation. User can select a range for fitting a straight line to calculate the electron temperature, as explained above. To properly operate the program, ranges of the slide bars would be initially defined automatically. We will discuss in the next section. This means that the manual analysis composed of two sub-processes, the automated algorithm for the initial definition, and the manual operation for the user one.

In result display, there are five indicators that present the plasma parameters, the plasma and floating potentials, the electron and ion densities, and the electron temperature. After all regions are set, results will be displayed on the screen. These results, including the definition, slopes and intercepts of each range, would be saved when the save bottom (in figure 3.5) is pressed. The example of the saved file is shown in table 3.1.

Table 3.1: The example of the save file.

| | | | |
|---|---|---|---|
| Floating potential (V) | | -3 | results |
| Plasma potential (V) | | 52.28 | |
| Electron density (1/mm^3)) | | 1.91E+09 | |
| Ion density (1/mm^3) | | 1.59E+09 | |
| Electron temperature (eV) | | 6.09 | |
| Smooth data points | | 1 | |
| Probe diameter (mm) | | 2.3 | |
| Probe length (mm) | | 0.85 | |
| Probe area (mm^2) | | 10.3 | |
| Ion mass (amu) | | 40 | |
| Start ion range (V) | | -30 | |
| End ion range (V) | | 12 | |
| m_i (A/V) | | 1.14E-06 | |
| c_i (A) | | 1.00E-05 | |
| Start transition range (V) | | 28 | |
| End transition range (V) | | 49 | |
| m_t (A/V) | | 1.20E-04 | |
| c_t (A) | | -3.00E-03 | |
| Start electron range (V) | | 64 | |
| End electron range (V) | | 90 | |
| m_e (A/V) | | 2.87E-05 | |
| c_e (A) | | 1.75E-03 | |
| Start Te range (V) | | 12 | |
| End Te range (V) | | 33 | |
| Ie,sat (A) | | 3.25E-03 | |
| V (V) | I (A) | ln Abs Ie | data |
| -30 | -1.70E-05 | -11.86 | |
| -29 | -1.65E-05 | -11.96 | |
| -28 | -1.61E-05 | -12.08 | |
| -27 | -1.56E-05 | -12.2 | |
| -26 | -1.51E-05 | -12.33 | |
| ⋮ | ⋮ | ⋮ | |

## 3.5 Automated Analysis

This section describes the process to analyze the I-V characteristic by the automated algorithm. From the manual analysis, a foreseeable obstruction for the automated process is to divide the I-V curve into three parts. After this problem is handled, the plasma parameters could be figured out. Figure 3.7 shows the flow chart of the algorithm to analyze the parameters. In figure 3.7, there are two programming subsection, the first one involve with the plasma analysis, and the other handle the file saving.

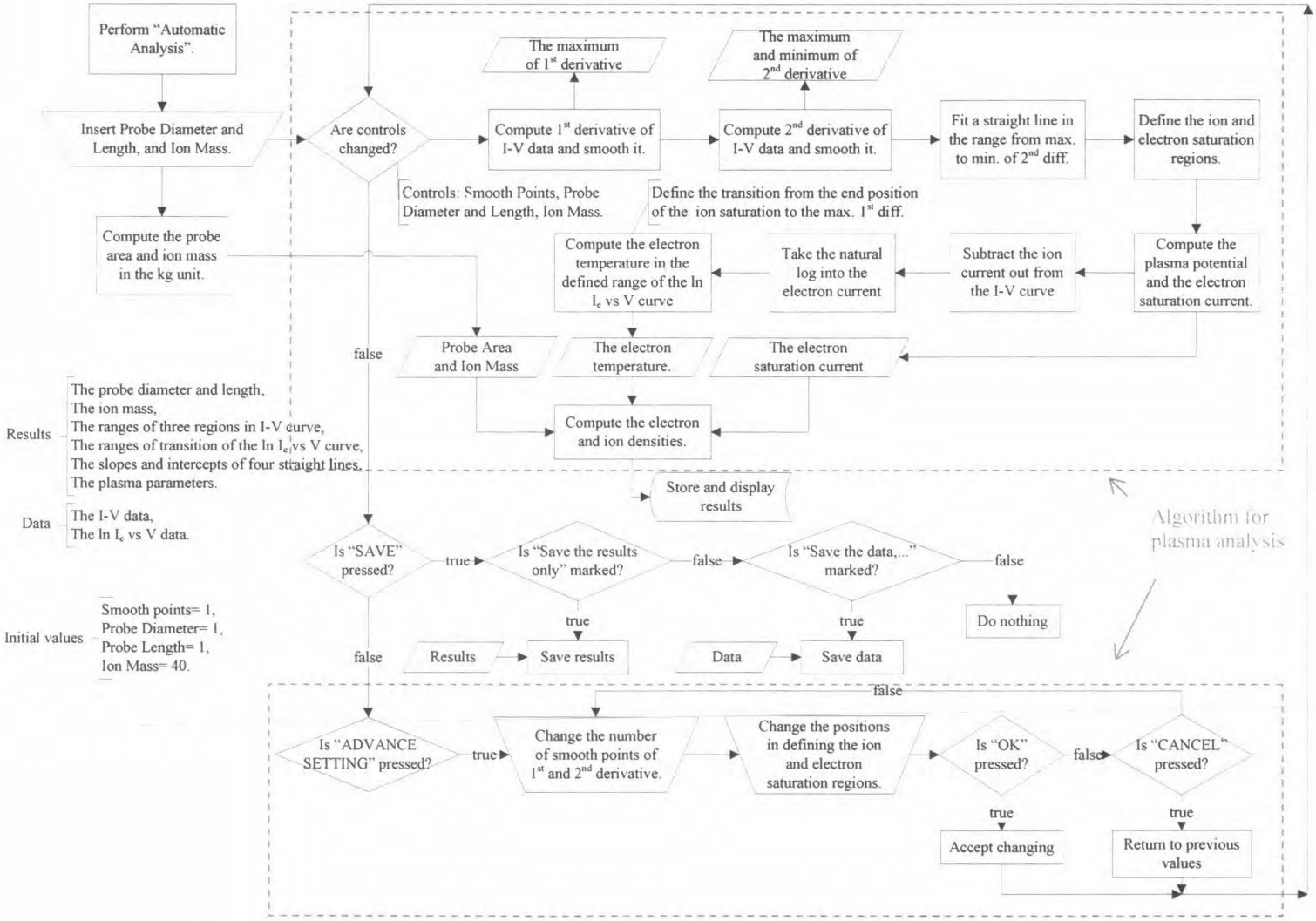


Figure 3.7: The flow chart of the algorithm to automatically analyze the parameters.

Before getting into the detail of how the algorithm works, there is a function that is important in our calculation and needed to be defined; this function is differentiation. The differentiated values in our work are calculated by averaging the slopes of two adjacent data set for each data as followed [20]:

$$\frac{1}{2}\left(\frac{y_{i+1}-y_i}{x_{i+1}-x_i}+\frac{y_i-y_{i-1}}{x_i-x_{i-1}}\right)$$

when $(x_i, y_i)$ is the data point at index $i$. In this work, we use the function for calculating the first and second derivatives of currents with respect to voltages, accompanying with the smoothing function. Because of the I-V characteristic, a maximum will appear by the first derivative, and if we take another differentiation, both maximum and minimum characteristics will arise. The smoothing algorithm will be used in reducing fluctuation after the differentiation.

When I-V data were taken in the algorithm, the program would calculate the first derivative of them. The derivative data would normally show fluctuation, lead to difficulty in finding the clear peak as seen in figure 3.8(a). After systematically trial in all the I-V data, we decided to use up to seven adjacent points for smoothing that was enough to alleviate the noise in figuring the maximum peak out. At the maximum position in figure 3.8(b), we kept data for the computation of the electron temperature. In the process of the derivative, one could see two horizontal lines on left and right sides of the maximum peak. These lines corresponded to the ion and electron saturation regions, which were used in defining these regions. These processes will be discussed after the next step, finding a straight line in the transition region.

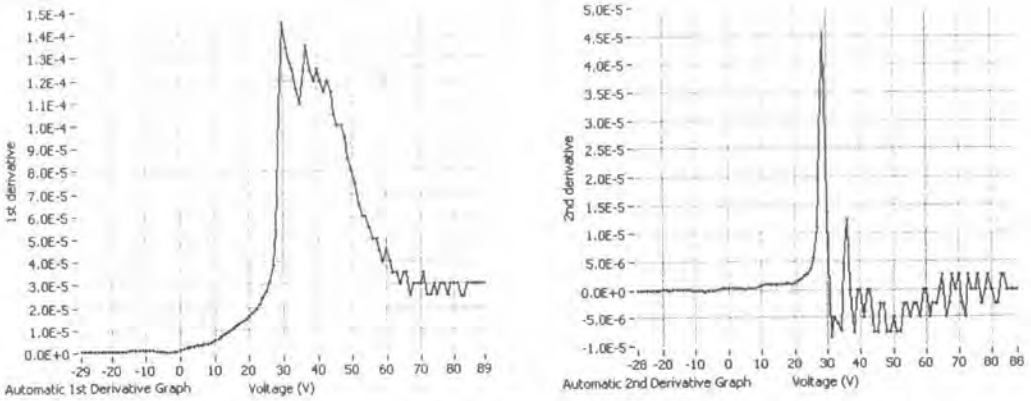


(a) No smoothing in the first and second derivatives.

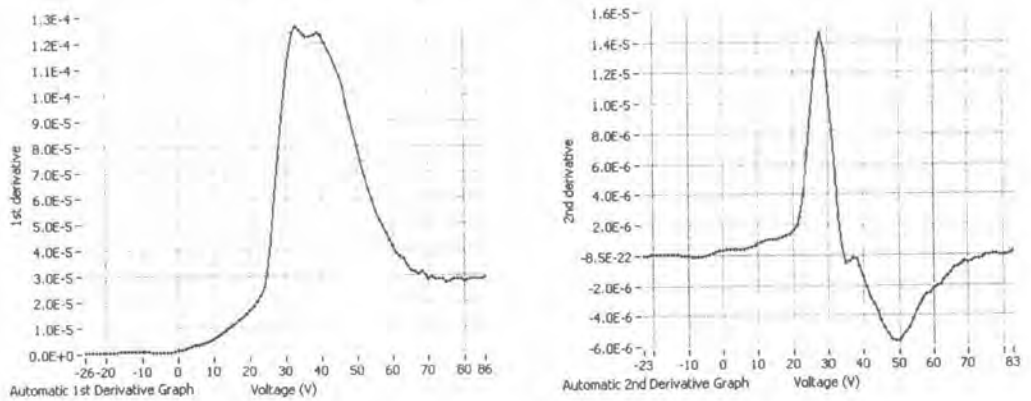


(b) Smoothing in the first and second derivatives.

Figure 3.8: The difference between (a) no smoothing and (b) smoothing in the first and second derivatives shows false positions in defining the maximum peak of the first derivation and the maximum and the minimum peaks of the second derivation in the figure (a) comparing with the figure (b).

After the first derivative, the algorithm would compute the second derivation and perform the smoothing. For the smoothing, the number of data up to five points would be averaged which yielded sufficient noise reduction of the derivative in figure 3.8(b). The range from the maximum to minimum positions was used to fit a linear line in the transition of the I-V curve. With this way, we could not isolate out the ion-saturation region at the maximum position and the electron-saturation at the minimum from the transition, and fit two straight lines in their regions. If it had done, the slope of the ion current would have been steeper than its slope that came from the ion-saturation, as seen in figure 3.9. This behavior would also be found in the electron-saturation if we used the minimum position of the second derivative to isolate the

electron-saturation from the transition region. Certainly, these problems can cause miscalculation in plasma parameters.

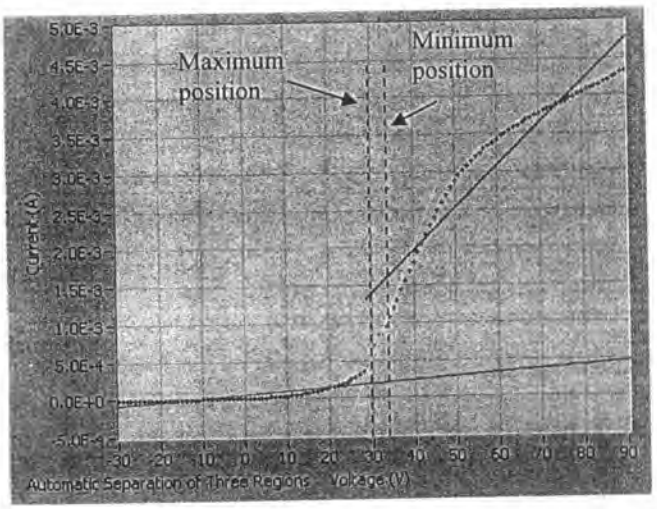


Figure 3.9: The effect of using the maximum and minimum peak of 2nd derivative without smoothing in separating the I-V curve into three regions and in fitting three straight lines in those regions.

In order to define appropriate ranges for fitting straight lines of current in the ion and electron saturation regions, the graph of the first derivative and the maximum and minimum of the second were taken into account, as illustrated in figure 3.10(a). The first and second derivatives were shown, where the solid curve represented the first and the dash was of the other. We used the range between the maximum and minimum for the straight line in the transition region. Thus outside of this range, the left of the maximum and the right of the minimum, were used to define the ion and electron saturation regions, respectively. The two vertical dash lines in figure 3.10(a) show three intervals, of which the left and right intervals are depicted in figure 3.10(b) and 3.10(c).

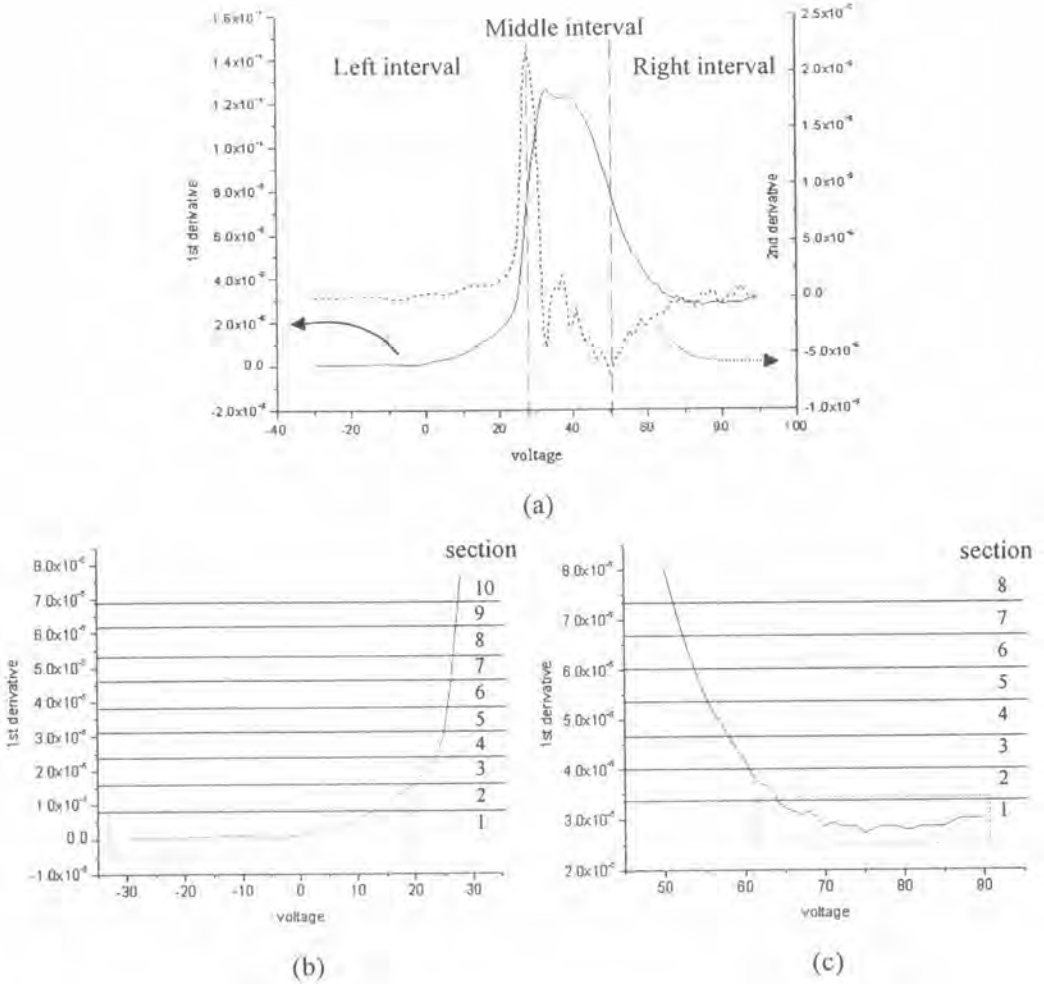


Figure 3.10: The process for isolating the ion and electron saturation regions, (a) dividing the 1st derivative at the maximum and minimum of the 2nd derivative, (b) and (c) dividing the curves into ten parts and eight parts, respectively.

For the ion-saturation region in figure 3.10(b), the curve was divided into ten sections in the first derivative. Most the derivative data stayed within section one which corresponded to the ion-saturation region. When voltages were more than 15 V in figure 3.10(b), the tendency of the derivative rapidly increased. At this position, the first derivative corresponded to the current of the I-V curve when the current approached the transition region. In the section one in figure 3.10(b), the derivative remained constant in correspondence with the ion-saturation region. Therefore, we used the range in this section to fit the linear line in the I-V curve as the ion current.

The electron-saturation region could follow the method in defining the ion-saturation region. The range of the electron-saturation was defined from the first

derivative in the section one, depicted in figure 3.10(c). For the range definition of the electron-saturation, we divided into eight parts because of fluctuation that came along with the derivative in the electron-saturation region. An example of this problem was depicted in figure 3.11. When current in the I-V curve (see the right figure of figure 3.11) reached the electron-saturation region, the current would fluctuate, unlike current in the ion-saturation region. The fluctuate current affected on the first derivative that resulted in the derivative to scatter in the electron-saturation region. If the more number parts we used, the less data we remained (see the left figure in figure 3.11). This led to unfit the linear line in this region (see the right figure). To avoid this problem which remained a few data points for fitting the straight line, we divided the first derivation into eight parts and defined the electron-saturation region in the section one from figure 3.10(c).

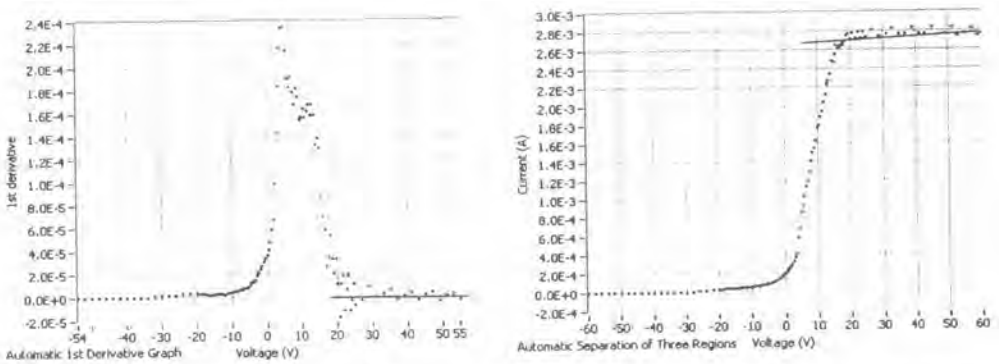


Figure 3.11: The effect of the electron-saturation definition on unfitting the straight line.

From the above explanation, we obtained three straight lines in each region, as shown in figure 3.12. The plasma potential then derived from the intercept of two straight lines in the transition and electron-saturation, and the electron-saturation current would obtain at the same time. For the ion density, the ion-saturation current ($I_{i,sat}$), which was used to compute the density, obtaining from the intercept of the ion current line at voltage equal to zero. And then the process for the plasma analysis followed: subtracting the ion current, and re-plotting the electron current, respectively.

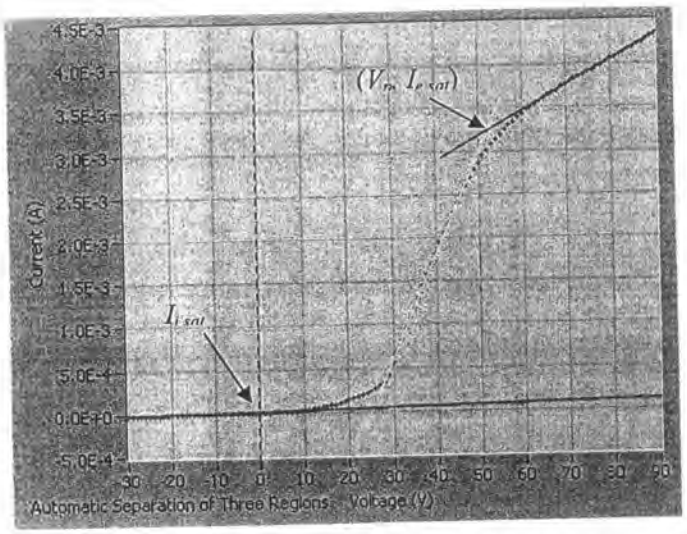


Figure 3.12: The result of separating ion, electron saturation and transition regions.

The calculation of the electron temperature for this automated algorithm was quit different from the manual calculation. Because the automated process had to define the range in ln $I_e$-$V$ curves to fit a straight line, and had to set the range which was nearly similar to the manual calculation. Figure 3.13 shows the graphs of current and voltage (the left figure) and of natural log of absolute electron current and voltage (the right figure), which contain four vertical lines in the two figures. Such lines correspond in voltage positions between the two graphs.

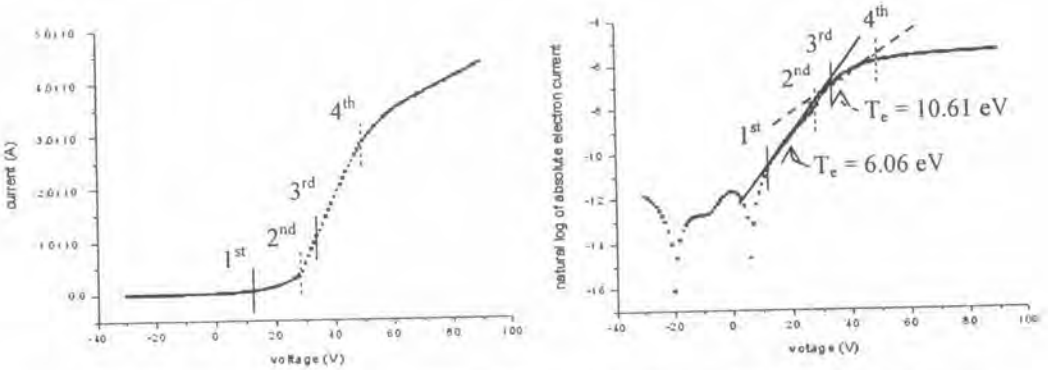


Figure 3.13: The overestimation of electron temperature because of the defined ranges between I-V curve and $\ln|I_e| - V$ curve.

From the right figure in figure 3.13, it would overestimate the temperature if we used the range between two dash lines (the second and the fourth lines) obtaining from the maximum and minimum of the second derivative. In the manual way for

fitting the straight line in the ln $I_e$-V curve, the end of the range was usually selected between the second and third lines [4,6,15,16,21], yet some research articles preferred to choose at the third, which was the maximum of the first derivative [9-11,22,23]. In these articles, the end of the electron temperature calculation was defined from the maximum of the first derivative. And the beginning of the range was defined at the floating potential where the current approaching zero. However, from experiments, it was inappropriate to use the floating potential because this potential located into the ion-saturation region. This occurred in some experiments, so we could not use the floating potential for all data. The better way to select the beginning of this range was to use the position that was defined the end of the ion-saturation, the first solid line, which obtained early.

To summarize, the automated algorithm imitating the manual calculation had to define appropriate ranges, and to estimate plasma parameters. All these processes used the characteristics of the first and second derivatives in different ways, as shown in table 3.2.

Table 3.2: Conclusion in defining the three regions and plasma parameters.

| | Definition |
|---|---|
| The floating potential ($V_f$) | The voltage at current approaching to zero. |
| The transition region | The range from the maximum to minimum peaks of the second derivative. |
| The ion-saturation region | Almost linear response on the left side of the maximum of the first derivative. |
| The electron-saturation region | Almost linear response on the right side of the maximum of the first derivative. |
| The ion current | Linear fitting in the ion-saturation region. |
| The ion-saturation current ($I_{i,sat}$) | The intercept of the ion current. |
| The plasma potential ($V_p$) and the electron-saturation current ($I_{e,sat}$) | The intercept of the two straight lines in the transition and the electron-saturation regions. |
| The electron temperature ($T_e$) calculation | Linear fitting in the range between the end of the ion-saturation region and the maximum of the first derivative. |
| The electron and ion densities ($n_e$ and $n_i$) | Calculating from equation (2.17) and (2.18), respectively. |

The user interface in LabVIEW, for this algorithm, is illustrated in figure 3.14. It consists of two windows which are shown in figure 3.14(a) for the result display and figure 3.14(b) for the advance setting. The appearance of the display is similar to that of the manual version (see figure 3.5), but with locks on some controls, and replaced with the advance setting bottom. When the advance setting is pressed, the result window will turn to the advance setting. This setting involves the definition of ranges for the ion and electron saturation regions and the smoothing adjacent points for the first and second differentiations. In this window, the default bottom will sets the values at the initial values, as explained early. When one of the values change, the ok bottom accepts the change, and the cancel returns to the previous change.

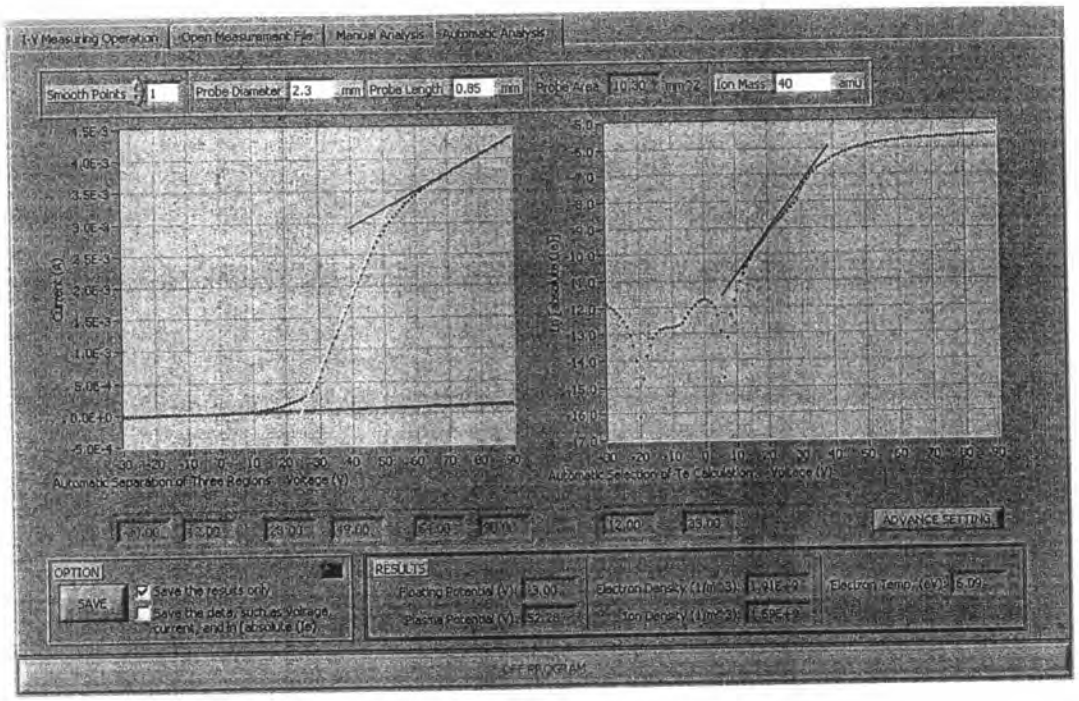


(a)

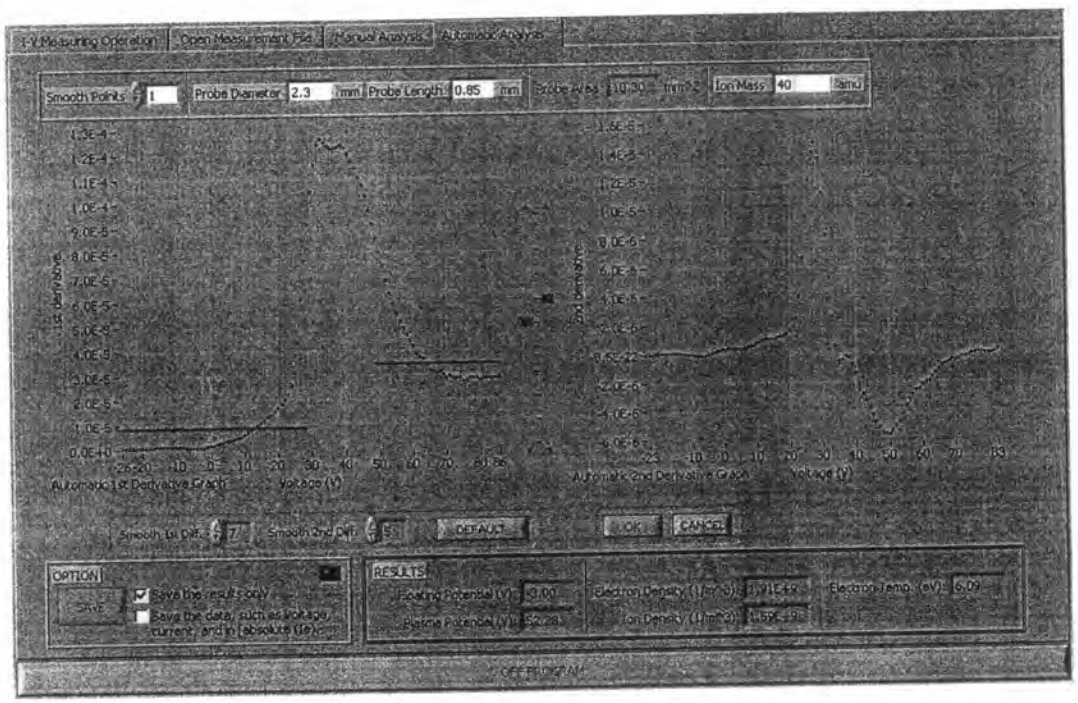


(b)

Figure 3.14: The user interface in LabVIEW of the automatic analysis, (a) the result display and (b) the advance setting.